Journal of Magnetism and Magnetic Materials 401 (2016) 217–222

Contents lists available at ScienceDirect

Journal of Magnetism and Magnetic Materials

journal homepage: www.elsevier.com/locate/jmmm

The superexchange interactions and magnetic ordering in low-dimentional ludwigite $Ni_5GeB_2O_{10}$

S.N. Sofronova [a,*], L.N. Bezmaternykh [a], E.V. Eremin [a,b], I.I. Nazarenko [b], N.V. Volkov [a,b], A.V. Kartashev [a], E.M. Moshkina [a,b]

[a] L.V. Kirensky Institute of Physics, Siberian Branch of Russian Academy of Science, 660036 Krasnoyarsk, Russia
[b] M.V. Reshetnev Siberian State Aerospace University, 660014 Krasnoyarsk, Russia

ARTICLE INFO

Article history:
Received 30 July 2015
Received in revised form
25 September 2015
Accepted 9 October 2015
Available online 20 October 2015

Keywords:
Ludwigites
Magnetic order
Heat capacity
Exchange interactions
Ferrimagnetic

ABSTRACT

The ludwigite $Ni_5Ge(BO_5)_2$ belongs to a family of oxyborates which have low-dimensional subunits in the form of three-leg ladders unit structure. This material was studied by magnetic and thermodynamic measurements. $Ni_5Ge(BO_5)_2$ does not show full long-range magnetic order, but one goes into a partial ordering or spin-glass state at 87 K. The superexchange interactions were calculated in the framework of a simple indirect coupling model. Different models of magnetic structure of $Ni_5Ge(BO_5)_2$ and its unique magnetic behaviour was discussed.

© 2015 Elsevier B.V. All rights reserved.

1. Introduction

The ludwigites M_3BO_5 belong to the anhydrous oxyborates. In these materials, the metal ions form substructures such as ribbons, ladders and zigzag walls. The ludwigites are good examples of strongly correlated low dimensional systems with interesting physical properties. There are a charge-ordering phenomenon, the existence of two magnetic subsystems ordering independently at different temperatures in orthogonal directions, a spin-glass magnetic ordering, a reversal magnetization in these materials [1–5].

The specific-heat measurements show the long-range magnetic ordering in the whole system only in homometallic ludwigites (Fe_3BO_5 and Co_3BO_5) [6,7], the exception is $Co_5Sn(BO_5)_2$ [8]. In the heterometallic compounds with a magnetic metal ions there are no a true thermodynamic magnetic transitions. The magnetic ordering of the Fe^{3+} ions is observed in Co_2FeBO_5 and Ni_2FeBO_5, but the magnetic moments of diavalent subsystem (Co or Ni) freeze at low temperatures [7–9]. Nonmagnetic ions (Ti^{4+}, Mg^{2+}, Ga^{3+}) destroy long-range magnetic order and lead to spin-glass freezing in $Co_5Ti(BO_5)_2$ [10], $CoMgGaBO_5$ [11]. As cited above, despite being doped by nonmagnetic ions, $Co_5Sn(BO_5)_2$ has long range magnetic order below 82 K which is, surprisingly, the highest critical temperature found so far in the ludwigites [8]. This critical temperature can be explained by the absence of double-exchange interactions, which are usually present in the ludwigites and that give rise to a strong competition.

In order to extend our understanding of the interactions mechanism in the transition metal ludwigites, it is necessary to investigate materials of $Ni_{3-x}Me_xBO_5$ family (Me = Ge, Ti, Sn, Mn, Ga, Al, Cr, V). Many of these compounds were grown [12–17] before but there is no information about its physical properties.

This paper is the first step in studying of $Ni_{3-x}Me_xBO_5$ family. We present the study of the magnetic and thermodynamic properties of $Ni_5Ge(BO_5)_2$. We discuss the possible magnetic orderings in $Ni_5Ge(BO_5)_2$ and compare it with other investigated ludwigites.

2. Synthesis and structure

The single crystals of $Ni_5Ge(BO_5)_2$ with a ludwigite structure were synthesized by the spontaneous crystallization method. The flux was prepared in a platinum crucible with the volume $V = 100\ cm^3$ at the temperature $T = 1100\ ^\circ C$ by sequential melting of reactants taken in a molar ratio $Bi_2Mo_3O_{12}$:B_2O_3:Li_2CO_3:NiO:GeO_2 = 1:2.4:2:1.14:0.23. The total mass of reactants was 71 g. In the prepared flux, the phase crystallizing within a sufficiently wide (about 40 °C) high-temperature range was $Ni_5Ge(BO_5)_2$ with the ludwigite structure. The saturation temperature of the flux was $T_{sat} = 970\ ^\circ C$.

* Corresponding author.
E-mail address: ssn@iph.krasn.ru (S.N. Sofronova).

http://dx.doi.org/10.1016/j.jmmm.2015.10.024
0304-8853/© 2015 Elsevier B.V. All rights reserved.

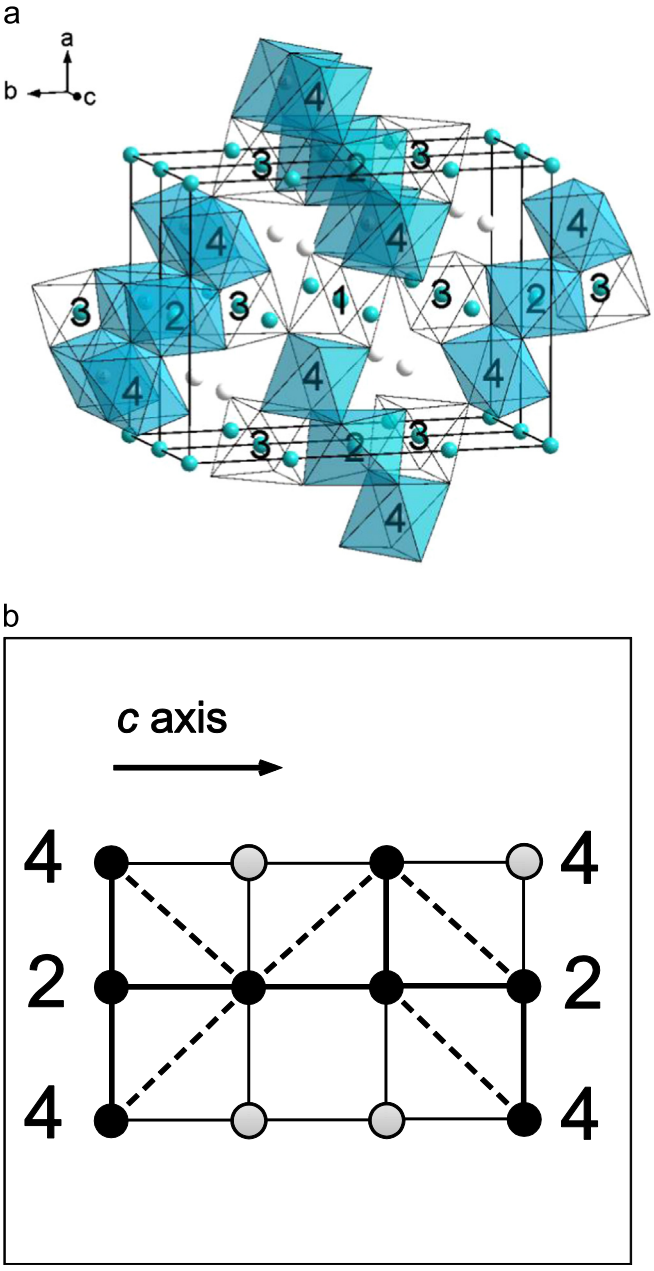

Fig. 1. (a) The structure of $Ni_5Ge(BO_5)_2$ crystal. (b) The subunit formed by the metal sites 4–2–4. The site 4 is occupied randomly by Ge and Ni ions in a proportion 0.5:0.5. Dark circles are Ni ions. The light circles are Ge ions. The 180° superexchanges are shown by the dashed lines. The 90° superexchanges are shown by the solid lines.

After homogenization of the flux at $T=1100$ °C for 3 h, the temperature was first rapidly reduced to $(T_{sat}-10)$ °C, and then slowly reduced with a rate of 4–12 °C/day. In 3 days, the growth was completed, the crucible was withdrawn from the furnace, and the flux was poured out. The grown single crystals in the form of black orthogonal prisms with a length up to 6 mm and a transverse size of about 0.3 mm were etched in a 20% water solution of nitric acid to remove the flux remainder.

A single-crystal x-ray diffraction of $Ni_5Ge(BO_5)_2$ showed that the structure of our single-crystals is the same as the structure was solved by Bluhm in the work [17]. We used the structural data from the Bluhm's paper [17]. The $Ni_5Ge(BO_5)_2$ crystal belongs to the $Pbam(D_{2h}^{16})$ space group with the lattice parameters $a=9.18$ Å, $b=12.14$ Å, and $c=2.98$ Å (Fig. 1). The unit cell involves two formula units. The sites 1(2b), 2(2c), 3(4h) are exclusively occupied by Ni. The site 4 (4g) is occupied randomly by Ge and Ni ions in a proportion 0.5:0.5 [17].

Table 1
The Ni–Ni bond lengths (Å) in $Ni_5Ge(BO_5)_2$.

Ni_i–Ni_j, i, j – crystallographic positions	R (Å)
Ni_4–Ni_4, Ni_1–Ni_1, Ni_2–Ni_2, Ni_3–Ni_3	2.98
Ni_4–Ni_3	3.084, 3.344
Ni_2–Ni_3	2.763
Ni_4–Ni_2	3.049
Ni_4–Ni_1	3.003
Ni_1–Ni_3	3.411

The ludwigite crystal structure consists of low-dimensional subunits: two three-leg ladders (3LLs) of different types. The ions in the 4–2–4 sites form so-called triads arranged as the rungs of the three-leg ladder of type I. Direct exchange is usually possible in the 4–2–4 ladders which have the smallest intermetallic distances (see Table 1). The Goodenough rule predicts that the 180° superexchange interaction Ni^{2+}–Ni^{2+} in triads of type I are strongly antiferromagnetic, as the 90° superexchange interaction Ni^{2+}–Ni^{2+} in triads of type I are ferromagnetic (Fig. 1(b)) [18]. The ions in the 3–1–3 sites form a three-leg ladder of type II. Triads of type II have the biggest intermetallic distances (see Table 1). The columns of edge-sharing octahedral form zigzag walls spreading along the crystallographic c axis.

3. Magnetic measurements

The magnetic measurements were performed using PPMS and MPMS facilities (Quantum Design) at the temperatures of 2–300 K in the magnetic fields up to 70 kOe. Figs. 2 and 3 present temperature dependences of magnetization and temperature dependences of inverse magnetic susceptibility of $Ni_5Ge(BO_5)_2$. Zero-field cooled (ZFC) and field cooled (FC) dc magnetization measurements were performed with applied fields of 1 kOe (Fig. 2) and 25 kOe (Fig. 3) oriented along the a, b, and c axes of single crystal. The magnetization curves have a sharp kink pointing out the occurrence of magnetic ordering near $T=87$ K. The temperature dependences of magnetization along the a and b axes show splitting of the curves corresponding to FC and ZFC regimes. The temperature dependence of the inverse dc magnetic susceptibility

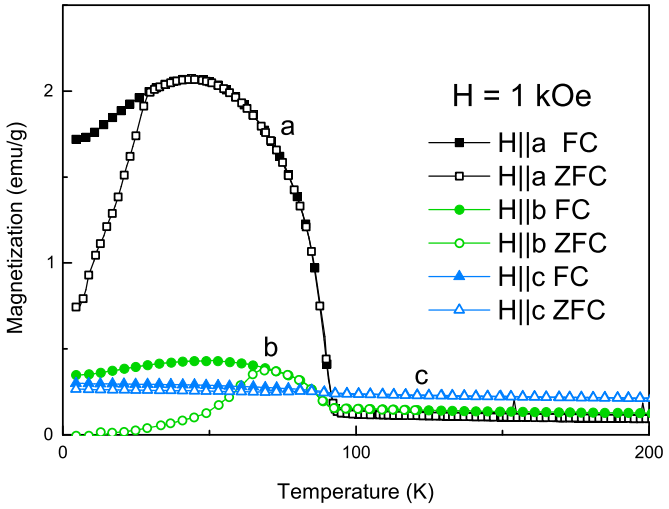

Fig. 2. The temperature dependences of magnetization in an applied field of 1 kOe oriented along the a, b, and c axes of single crystal in both regimes: zero-field cooled (ZFC) and field cooled (FC).

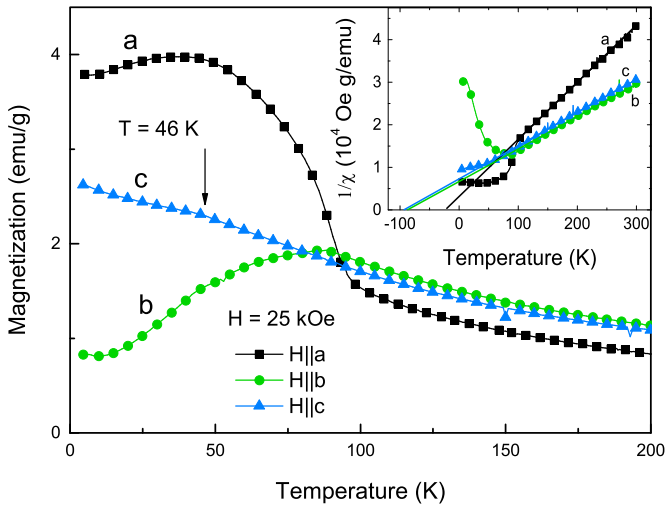

Fig. 3. The temperature dependences of magnetization in an applied field of 25 kOe oriented along the *a*, *b*, and *c* axes of single crystal. The inset shows the temperature dependences of inverse magnetic susceptibility.

along the *b*, *c* axis above 87 K is close to linear as the Curie–Weiss law predicts. The temperature dependence of the inverse dc magnetic susceptibility along the *a* axis above 120 K is close to linear. We have $\theta_a = -23$ K. In the other directions, the Weiss temperature has a high modulus and a negative value ($\theta_{b,c} \sim -90$ K), which indicate predominant antiferromagnetic interactions. The effective magnetic moments μ_{eff} calculated for the paramagnetic phase per formula unit in directions *b* and *c* are close to each other (the difference is about 3%) $-5.48\ \mu_B$ and $5.36\ \mu_B$, respectively, as the effective magnetic moments μ_{eff} in direction *a* – $4.05\ \mu_B$. The spin component of the effective moment $\mu = 2gS(S+1)$ is $4.47\ \mu_B$. We assumed that the Ni^{2+} ions are in the high-spin state $S=1$ and *g* factor was taken to be 2. The effective magnetic moment is $\mu = 2gJ(J+1) = 14.13\ \mu_B$ per formula unit if the orbital component is taken into account. Comparing the calculated values of μ_s and μ_J with the experimental value μ_{eff}, one can see that the spin value μ_s is closer to μ_{eff} than μ_J.

The magnetic measurements indicate that the $Ni_5Ge(BO_5)_2$ is extremely anisotropic. A magnetic anisotropy manifests itself clearly in the paramagnetic state, which is obvious from the sharp difference in the Weiss temperatures as a function of the magnetic field direction. The same behaviour was found in Co_3BO_5 [9], where the paramagnetic anisotropy can be explained by strong spin-lattice effects due to the spin-orbit stabilization of $Co^{2+}(d7)$ ions in octahedral sites. The same effects could appear if Ni^{2+} $(d8)$ ions are in a tetrahedral sites, but Ni^{2+} ions are in octahedral sites in the ludwigite structure. In the ludwigite structure, ions of Ni^{2+} are not expected to be active in a spin-lattice sense.

The measurements ac magnetic susceptibilities are shown dependency of the magnetic susceptibility with the frequency.

Fig. 4 presents field dependences of magnetization along the *a*, *b*, and *c* axes obtained at different temperatures. At 100 K the magnetization exhibits a paramagnetic behaviour. Below T_c the hysteresis loops appear on magnetization curves along *a* and *b* axes. The hysteresis loops along *a* axis have the form of parallelograms. The loop at 50 K has the exchange bias. Surprisingly, but the exchange bias vanishes when the temperature decreases. The existence of the exchange bias can evidence that the $Ni_5Ge(BO_5)_2$ is the material with competing magnetic interactions, where due to the arrangement of the magnetic ions, different areas (or domains) with AFM or FM interactions are created. The exchange bias effects have been observed in spin glass systems and some ferrimagnets [19]. Usually the exchange bias vanishes above the

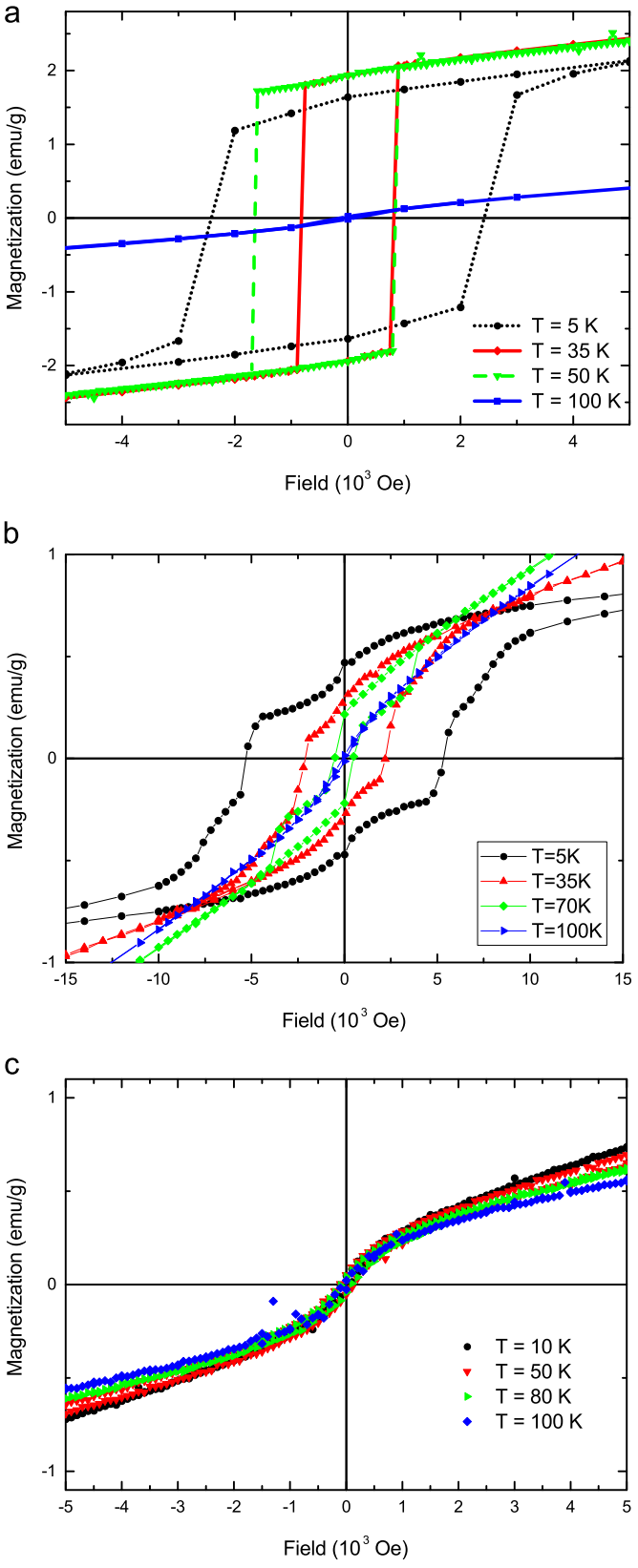

Fig. 4. Magnetization isotherms for $Ni_5Ge(BO_5)_2$ along the *a*, *b*, and *c* axes of single crystal below and above the magnetic transition.

'blocking' temperature or the Neel temperature [19]. There are some feature at $T=46$ K on magnetization curves (Fig. 3). We assume that the magnetic order in $Ni_5Ge(BO_5)_2$ changes when the temperature decreases and below $T=46$ K the exchange bias

vanishes.

For the field directed along the axis *b*, the hysteresis loop presents small jumps or plateaus of magnetization. The similar behaviour was also found in $Co_5Ti(BO_5)_2$ [10] and in this case it related to a spin-glass phase. In case of magnetically ordered $Co_5Sn(BO_5)_2$ [8], the magnetization jumps are associated with metamagnetic behaviour.

4. Specific-heat measurements

Specific-head measurements as a function of temperature and magnetic field were performed employing 14.7 mg of crystals. The same PPMS platform Quantum Design equipment was used. Fig. 5 shows the specific-heat curves with and without an applied magnetic field of 25 kOe. $Ni_5Ge(BO_5)_2$ has a sharp peak at 87 K similar to that observed in Ni_2FeBO_5 or Co_2FeBO_5 [7]. We notice that the peak at 87 K is not changed with the applied magnetic field. In magnetically ordered Co_3BO_5 and $Co_5SnB_2O_{10}$ the peak is smoothed down with the applied magnetic field [6,8]. To describe

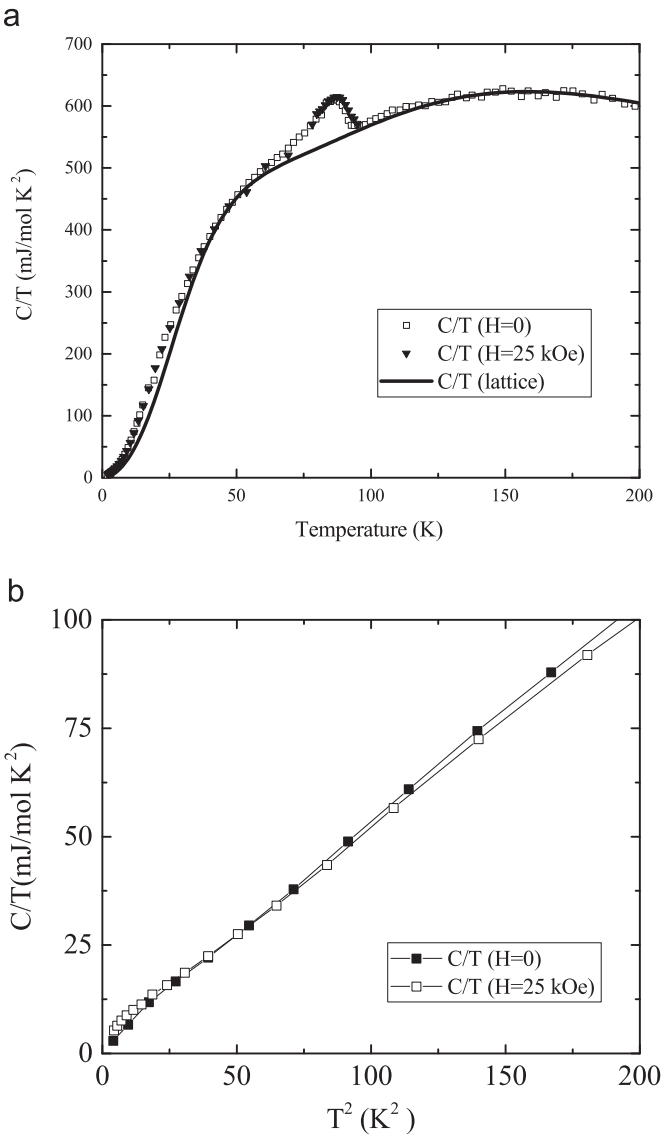

Fig. 5. (a) The specific-heat curves with (triangles) and without (bars) an applied magnetic field of 25 kOe. The solid line shows the lattice contribution of the heat capacity. (b) The specific heat plotted as C/T versus T^2 for applied field 0 and 25 kOe.

lattice heat capacity $C_L(T)$, we used the combination of the Debye $C_D(\Theta_D/T)$ and Einstein $C_E(\Theta_E/T)$ functions. The best result was obtained at $\Theta_D=233$ K and $\Theta_E=566$ K. Excluding the lattice contribution of the heat capacity from the experimental data, we found the entropy of the magnetic transition $\Delta S=1.3$ J/mol K. This quantity is much less than the maximally possible magnetic entropy $\Delta S = 5/2R \ln(2S + 1) = 22.8$ J/mol K per one formula unit (5 Ni^{2+} ions with spin $S=1$ per two formula unit). The peak in the specific-heat curves is not associated with a full ordering of all magnetic moments. We assume that the magnetic behaviour of $Ni_5Ge(BO_5)_2$ corresponds to a freezing of the moments of part of ions or spin-glass state.

At the lowest temperatures we fitted the specific heat using a $C/T=\gamma+\beta T^2$ law for a magnetic field of 25 kOe and in zero field (Fig. 5(b)). The result of the fits yields a value for the coefficient γ:$\gamma(H=0)=1.7$ mJ/(mol K^2) and $\gamma(H=25$ kOe$)=3.8$ mJ/(mol K^2). For the coefficients of the T^3 term they yield $\beta(H=0)=0.52$ mJ/(mol K^4) and $\beta(H=25$ kOe$)=0.49$ mJ/(mol K^4). The parameters γ and β are similar to γ and β parameters of Co_2FeBO_5 [7].

The main feature of the ludwigites is the existence of a linear-dependent contribution to the specific heat. In insulating materials (the oxyborates are generally semiconductors or insulators at low temperatures) this linear term can be attributed to disorder due to magnetic frustrations.

The specific heat measurements, the exchange bias and the magnetization jumps confirm our conclusions that the magnetic behaviour of this compound corresponds to a freezing of the moments of part of ions or spin-glass state.

5. Indirect coupling model

In the ludwigites there is a competition between three types of magnetic interactions: direct exchange, superexchange and double exchange [8]. To analyze the magnetic structures and estimate the superexchange interactions in $Ni_5Ge(BO_5)_2$ crystal, we used a simple indirect coupling model [20,21] based on the theory of the super-exchange interaction of Anderson and Zavadskii [22] and Eremin [23]. Within the indirect coupling model, the structure of the crystals can be characterized by the following integrals of the indirect exchange coupling with regard to occupations of individual cation orbitals and symmetries of the lattice of indirect couplings $J_{ij}^{\alpha\beta}$, where i and j are the numbers of nonequivalent crystallographic positions for magnetic ions and α, β are the angles of the indirect coupling between magnetic ions.

The calculated exchange integrals for $Ni_5Ge(BO_5)_2$ are presented in Table 2.

Here, b and c are the electron transfer parameters being squares of ligand-cation intermixing coefficients for the σ and π coupling, respectively (the values of these parameters are $b=0.02$ and $c=0.01$); U (Ni^{2+})$=2.7$ eV is the cation-ligand excitation energy; J^{in} (Ni^{2+})$=2$ eV is the integral of the interatomic exchange interaction [20,21].

One can be seen from Table 2, the superexchange $J_{4-2}^{180^\circ}$ is strong and antiferromagnetic, that is in agreement with Goodenough rule. The superexchanges between zig-zag walls ($J_{3-4}^{120^\circ}$ and $J_{3-1}^{120^\circ}$) are weak and antiferromagnetic. All other 90° superexchanges are ferromagnetic.

Study of Fe_3BO_5, Ni_2FeBO_5 and Co_2FeBO_5 showed that at first the magnetic order in ludwigites appears in the three-leg ladders of type I. In $Ni_5Ge(BO_5)_2$ the site 4 of the three-leg ladders of type I is occupied randomly by Ge and Ni ions in a proportion 0.5:0.5, that can influence the magnetic ordering. The ferromagnetic superexchange between ions in the site 3 and ions in triad I also can influence the magnetic ordering in the three-leg ladders of type I.

Table 2
The calculated value of superexchange integrals.

Crystallographic positions of interacting magnetic ions	The angles of the indirect coupling between magnetic ions	The superexchange integrals	The value of superexchange integrals (K)
4–2	$\alpha=165^\circ$	$J_{4-2}^{180^\circ} = -\frac{8}{9}b^2U_{Ni}\lvert\cos\alpha\rvert$	−11.0
4–4	$\alpha=93^\circ$ $\beta=99^\circ$	$J_{ij}^{90^\circ} = \frac{2}{3}bcJ_{Ni}(\sin\alpha+\sin\beta)$	5.5
3–3	$\alpha=90.4^\circ$ $\beta=91^\circ$		
2–2	$\alpha=\beta=92^\circ$		
1–1	$\alpha=\beta=91^\circ$		
4–2	$\alpha=\beta=84^\circ$		
4–3	$\alpha=95^\circ$ $\beta=99^\circ$		
4–1	$\alpha=92^\circ$ $\beta=98^\circ$		
4–3	$\alpha=117^\circ$	$J_{ij}^{120^\circ} = \frac{2}{3}b(cJ_{Ni}\sin\alpha-\frac{4}{3}bU_{Ni}\lvert\cos\alpha\rvert)$	−1.4
3–1	$\alpha=121^\circ$		−1.8

Let us consider the ordering in the three-leg ladders of type I and in the site 3. The magnetic moments in the three-leg ladders of type I cannot be oriented without competing exchange interactions. We consider two cases.

In first case, we assume that the main superexchanges are $J_{4-2}^{180^\circ}$, $J_{i-i}^{90^\circ}$, which mainly form the magnetic order. Arrows indicate the magnetic ordering imposed by these couplings (see also Fig. 6). In the present case, ladders I are formed by antiferromgnetically coupled ferromagnetic chains along *c*. The magnetic moments of ions in the site 3 also are formed by ferromagnetic chain along *c*. The superexchanges between ions in the site 3 and ions in triad I are frustrated. We propose that ferromagnetic chains formed by moments of ions in the site 3 and ferromagnetic chains formed by moments of ions in the site 2 are ferromagnetically coupled, because nonmagnetic Ge ions reduce coupling between ions in the site 4 and in the site 3.

The ferromagnetically coupled 3LL-I with moments of ions in the site 1 form the ferrimagnetic zigzag walls. The superexchanges between the zigzag walls are antiferromagnetic. In present case the magnetic cell coincides with the crystallographic one. All moments are aligned along the *a* axis. The total magnetic moment per unit cell is 0.5 μ_B in this case. We assume that the frustration could be the cause of canting of the magnetic moment in the site 3 along the *b* axis (Fig. 7).

In second case, the main superexchanges are J_{4-2}. Arrows indicate the magnetic ordering imposed by these couplings (see also Fig. 8). In the present case, ladders I are formed by ferromagnetically coupled antiferromagnetic chain along *c*. The magnetic moments of ions in the site 3 are formed by ferromagnetic chains along *c*. The superexchanges between ions in the site 3 and ions in triad I are frustrated (Fig. 8).

We propose that in the present case the magnetic structure will

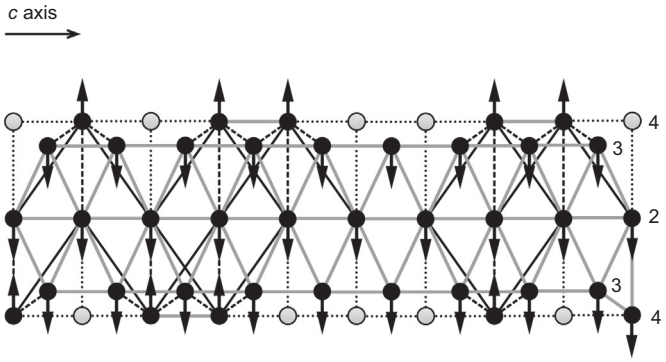

Fig. 6. The first type of magnetic order in the ladders I and the site 3. The dark circles are Ni ions. The open circles are Ge ions. The grey solid lines show the ferromagnetic superexchanges. The black solid lines show the antiferromagnetic superexchanges. The dashed lines show the frustrated interaction.

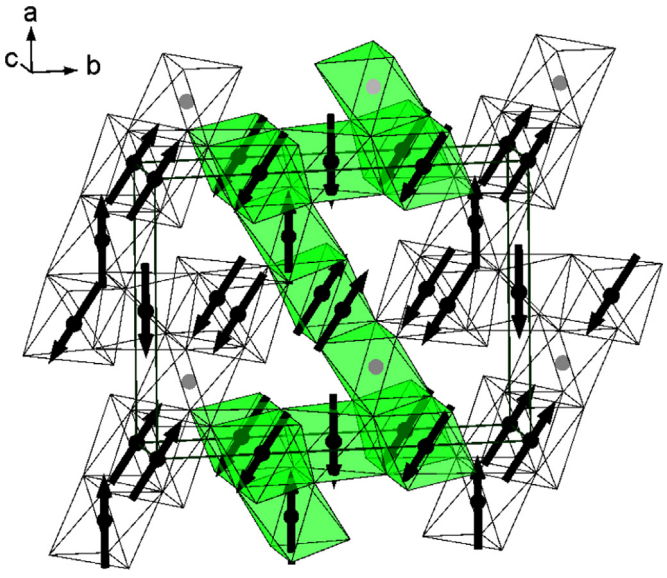

Fig. 7. The first type of magnetic ordering in $Ni_5Ge(BO_5)_2$.

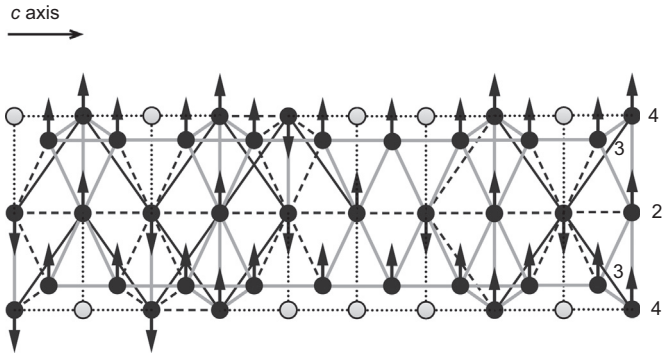

Fig. 8. The second type of magnetic order in the ladders I and the site 3. The dark circles are Ni ions. The open circles are Ge ions. The grey solid lines show the ferromagnetic superexchanges. The black solid lines show the antiferromagnetic superexchanges. The dashed lines show the frustrated interaction.

be similar to the magnetic structure of Fe_3BO_5. There are two magnetic subsystems oriented in orthogonal directions: ladders I form antiferromagnetic chains along the *c* axis, which are coupled ferromagnetically, ladders II form ferromagnetic chains along the *c* axis, which are coupled antiferromagnetically. In ladders I the moments are aligned along the *a* axis. In ladders II the moments are aligned along the *b* axis. The interactions between the same type of ladders are the supersuperexchange Ni–O–B–O–Ni. The interactions between the different types of ladders are frustrated. The proposed magnetic structure is shown in Fig. 9.

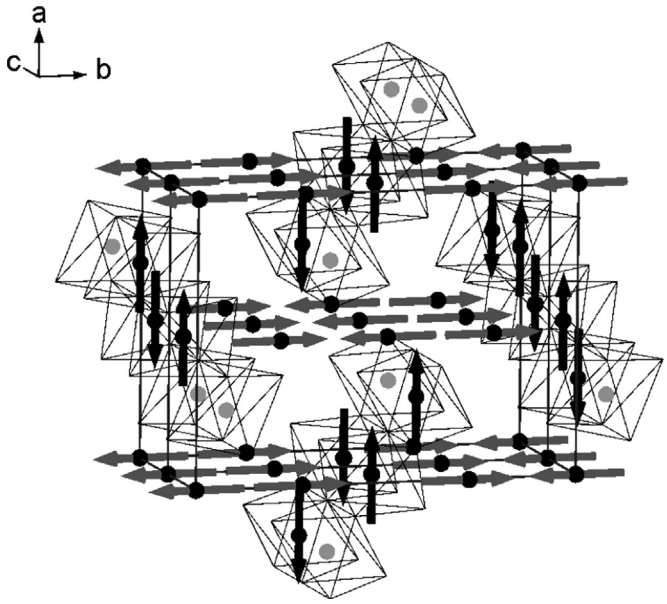

Fig. 9. The second type of magnetic ordering in $Ni_5Ge(BO_5)_2$.

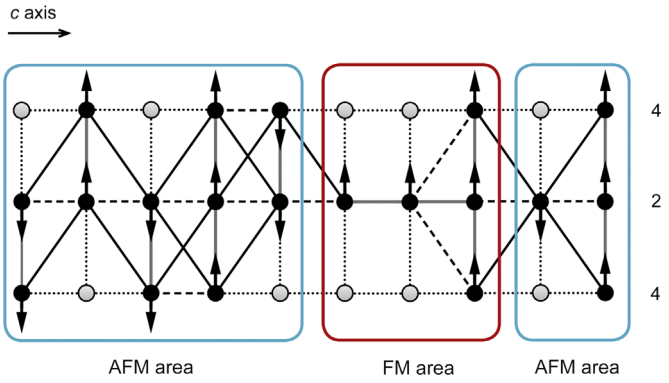

Fig. 10. Ferromagnetically and antiferromagnetically ordered areas in the ladders I. The dark circles are Ni ions. The open circles are Ge ions. The grey solid lines show the ferromagnetic superexchanges. The black solid lines show the antiferromagnetic superexchanges. The dashed lines show the frustrated interaction.

6. Conclusions

We propose that $Ni_5Ge(BO_5)_2$ is the material without well defined magnetic ordering. In this material there are competing magnetic interactions, where due to the arrangement of the magnetic ions, different areas with AFM or FM interactions are created. The specific heat measurements confirm our conclusions that the magnetic behaviour of this material corresponds to a freezing of the moments of part of ions or spin-glass state. The peak in the specific heat curves are not associated with a true thermodynamic magnetic transition. The exchange bias of hysteresis loops and "jumps" on hysteresis loops confirm the same magnetic behaviour. The calculation of the exchange interactions within a simple indirect coupling model shows that in this compound there is a competition between the ferromagnetic and antiferromagnetic exchange interactions.

We propose two models of magnetic ordering in $Ni_5Ge(BO_5)_2$. The common feature of both models is the magnetic order in the ladders II. The ladders II form ferromagnetic chains along the *c* axis which are coupled antiferromagnetically. There are no long range magnetic ordering in ladders I because there are competing magnetic interactions and the Ge ions which occupied randomly the site 4 influence to the magnetic order. In ladders I Ge-rich areas are ferromagnetically ordered (Fig. 10) but there are many frustrating interactions in Ni-rich areas. A surprising feature in present experiment is that the exchange bias vanishes when the temperature decreases. We assume that the competing magnetic interactions change the magnetic ordering in the ladders I when the temperature decreases.

However, the available experimental and theoretical data are still lack to establish the magnetic structure of the compounds under study and to describe all the features, in particular, the strong anisotropy in the paramagnetic phase. Clarification of the magnetic structure and mechanisms of the phase transitions in these compounds requires additional studies.

Acknowledgements

This study was supported by Russian Foundation for Basic Research (RFFI Siberia No. 15-42-04186). We thank S. Popkov, G. Yurkin for help on the magnetic measurements and M.S. Molokeev for help on the x-ray diffraction.

References

[1] E. Bertaut, Acta Crystollogr. 3 (1950) 473.
[2] H. Neuendorf, W. Gunser, JMMM 173 (1997) 117.
[3] P. Bordet, E. Suard, Phys. Rev. B 79 (2009) 144408.
[4] L.N. Bezmaternykh, E.M. Kolesnikova, E.V. Eremin, S.N. Sofronova, N.V. Volkov, M.S. Molokeev, JMMM 364 (2014) 55.
[5] L. Bezmaternykh, E. Moshkina, E. Eremin, M. Molokeev, N. Volkov, Y. Seryotkin, Sol. St. Phen. 233–234 (2015) 133.
[6] D.C. Freitas, M.A. Continentino, R.B. Guimarães, J.C. Fernandes, J. Ellena, L. Ghivelder, Phys. Rev. B 77 (2008) 184422.
[7] D.C. Freitas, M.A. Continentino, R.B. Guimarães, J.C. Fernandes, E.P. Oliveira, R. E. Santelli, J. Ellena, L. Ghivelder, Phys. Rev. B 79 (2009) 134437.
[8] C.P. Contreras Medrano, D.C. Freitas, D.R. Sanchez, C.B. Pinheiro, G.G. Eslava, L. Ghivelder, M.A. Continentino, Phys. Rev. B 91 (2015) 054402.
[9] N.B. Ivanova, N.V. Kazak, Yu. V. Knyazev, D.A. Velikanov, L.N. Bezmaternykh, S. G. Ovchinnikov, A.D. Vasiliev, M.S. Platunov, J. Bartolomé, G.S. Patrin, JETP 113 (2011) 1015.
[10] D.C. Freitas, R.B. Guimarães, R.D. Sanchez, J.C. Fernandes, M.A. Continentino, J. Ellena, A. Kitada, H. Kageyama, A. Matsuo, K. Kingo, G.G. Eslava, L. Ghivelder, Phys. Rev. B 81 (2010) 024432.
[11] N.B. Ivanova, M.S. Platunov, Yu. V. Knyazev, N.V. Kazak, L.N. Bezmaternykh, E. V. Eremin, A.D. Vasiliev, Low Temp. Phys. 38 (2012) 172.
[12] K. Bluhm, Hk Muller-Buschbaum, Z. Anorg. Allg. Chem. 582 (1990) 15.
[13] J.A. Hriljac, R.D. Brown, A.K. Cheetham, L.C. Satek, J. Solid State Chem. 84 (1990) 289.
[14] R. Norrestam, M. Kritikos, K. Nielsen, I. Søtofte, N. Thorup, J. Solid State Chem. 111 (1994) 217.
[15] C.G.F. Stenger, G.C. Verschoor, D.J.W. Ijdo, Mater. Res. Bull. 8 (1973) 1285.
[16] K. Bluhm, Hk Muller-Buschbaum, Z. Anorg. Allg. Chem. 579 (1989) 111.
[17] K. Bluhm, Hk Muller-Buschbaum, J. Less Common Met. 147 (1989) 133.
[18] J.B. Goodenough, Phys. Rev. 117 (1960) 1442.
[19] J. Nogues, I.K. Schuller, JMMM 192 (1999) 203.
[20] O.A. Bayukov, A.F. Savitskii, Phys. Stat. Sol. (B) 155 (1989) 249.
[21] O.A. Bayukov, A.F. Savitskii, Fiz Tverd. Tela 36 (1994) 1923.
[22] P.W. Anderson, Phys. Rev. 115 (1959) 2.
[23] M.V. Eremin, Fiz Tverd. Tela 24 (1982) 423.